Tikrit Journal of Pure Science Vol. 31 (3) 2026

DOI: *https://doi.org/10.25130/tjps.v31i3.1902*

IRAQI Academic Scientific Journals

Tikrit Journal of Pure Science

ISSN: 1813 – 1662 (Print) --- E-ISSN: 2415 – 1726 (Online)

Journal Homepage: https://tjpsj.org/

Investigation of Hydraulic Conductivity and Infiltration Capacity in Qushtapa and Shamamik Area in Erbil Basin, Kurdistan Region, Iraq

Seber M. M. Ameen[1], **Rebwar N. Dara**[2]

[1]*General Directorate of Divan, Ministry of Agriculture and Water Resources, Erbil, Kurdistan Region, Iraq*

[2]*Department of Earth Sciences and Petroleum, College of Science-Salahaddin University - Erbil, Kurdistan Region, Erbil, Iraq*

Received: 8 Feb. 2025 **Received in revised forum:** 25 May. 2025 **Accepted:** 1 Jun. 2025

Final Proofreading: 12 Jun. 2025 **Available online:** 25 Jun. 2026

ABSTRACT

This study examined soil hydraulic conductivity and infiltration capacity in the Qushtapa and Shamamik areas of the Erbil Basin. This study used the double-ring infiltrometer to measure soil infiltration capacity, grain-size analysis to determine soil textural characteristics, and the Hazen equation to derive soil hydraulic conductivity. Twenty infiltration tests and soil sample collections were done at the same location to assess the variability of these parameters across the study region. The results indicated that infiltration capacity was higher in soil samples with greater effective diameter (d10) and, consequently, showed higher hydraulic conductivity (K). The constant infiltration capacity ranged between 0.9 cm/h in Shamamik and 6 cm/h in Qushtapa. The infiltration results were close to those predicted by the Horton model. The soil of the investigated sites was classified as moderately to highly permeable. The findings of this study provide substantial data for irrigation and agricultural practices, land use planning, and best practices for sustainable water resource management in the region.

Keywords: Double ring, Effective diameter, Infiltration rate, Soil texture.

Name: Seber M. M. Ameen **E-mail:** sebarameen@gmail.com

Tikrit Journal of Pure Science Vol. 31 (3) 2026
DOI: https://doi.org/10.25130/tjps.v31i3.1902

دراسة التوصيلية الهيدروليكية وقدرة التسرب في منطقة قوشتبة وشمامك في حوض أربيل، إقليم كوردستان، شمال العراق

سيبر محسن محمد أمين [1،2]، ريبوار ناصر دارا [2،3]

[1] المديرية العامه للديوان، وزارة الزراعة والموارد المائية، اربيل، اقليم كورستان، العراق

[2] قسم علوم الارض والنفط، كلية العلوم، جامعة صلاح الدين-اربيل، اربيل، اقليم كوردستان، العراق

[3] قسم هندسة النفط، كلية الهندسة، جامعة نولج، أربيل، العراق

الملخص

تتناول هذه الدراسة معدل سعة التسرب والتوصيل الهيدروليكي للتربة في منطقتي قوشتبة وشمامك ضمن حوض أربيل. استخدمت هذه الدراسة طريقة مقياس الترشيح المزدوج الحلقة لقياس قدرة التربة على الترشيح، في حين تم إجراء تحليل حجم الحبوب لتحديد الخصائص التركيبية للتربة وتم اشتقاق التوصيل الهيدروليكي للتربة باستخدام معادلة هيزن. تم إجراء عشرين اختبار تسرب وجمع عينات التربة في نفس الموقع لتقييم تباين هذه المعلمات عبر منطقة الدراسة. أشارت النتائج إلى أن سعة التسرب أعلى في عينات التربة ذات القطر الفعال (d_{10})الأكبر، وبالتالي تظهر موصلية هيدروليكية (K) أعلى. تراوحت سعة التسرب الثابتة بين حد أدنى 0.9 سم / ساعة في شامامك وحد أقصى 6 سم / ساعة في قوشتبة. كانت نتائج قياسات التسرب قريبة من النموذج الذي صممه هورتون. تصنف تربة منطقة الدراسة على أنها تربة متوسطة وعالية النفاذية. توفر نتائج هذه الدراسة بيانات جوهرية لممارسات الري والزراعة، وتخطيط استخدام الأراضي، وأفضل الممارسات لإدارة موارد المياه المستدامة في المنطقة.

INTRODUCTION

Hydraulic conductivity and infiltration capacity influence water movement through the soil. They play an important role in hydrogeological processes, such as groundwater recharge, runoff, and soil degradation. Soil properties, including hydraulic conductivity, moisture content, texture, porosity, organic matter content, and chemical characteristics, mainly determine the infiltration rate. [1]. Water that infiltrates into the soil is a crucial source of groundwater for springs and wells, and sustains plant development. [2, 3]. The particle-size distributions of soil can vary significantly, leading to differences in infiltration rates among soil types.[4, 5].

Infiltration rate is an element in various hydrological procedures, including forecasting of surface runoff, prediction of groundwater recharge, managing watersheds, evaluation of water availability for plant growth, assessment of soil permeability, design of drainage and irrigation systems, forecasting of flooding, as well as erosion and estimation of runoff and maximum water discharge. [6-8].

There are three primary ways to conduct simple, rapid, and precise measurements of infiltration behavior: ring infiltrometer methods (single- or double-ring), the permeameter method, and sprinkler methods. [9, 10]. Researched the Bashtapa sub-basin, measured soil infiltration capacity in 15 locations by using a double-ring infiltrometer and applying Horton's equation. The results showed that infiltration capacity ranged from slow-moderate to moderate-rapid. Previously, [11] investigated the infiltration capacity of various soils at 17 sites within central Erbil Plain, using the double-ring method and applying Horton's equation. Their study divided the Erbil Plain into three zones based on the infiltration rate: low-moderate, moderate, and moderate-high.

Previous studies have sought to quantify infiltration rates regardless of how particle-size distribution influences hydrogeological conductivity. The climate of the area in the present study is classified as dry to semi-arid. The area faces significant challenges related to water scarcity, driven by climatic conditions, land-use changes, rapid population growth, and agricultural practices, all of which worsen water shortages for agricultural, industrial, and domestic uses. The lack of a comprehensive study of hydraulic conductivity and infiltration capacity in the region has impeded the development of essential water management strategies. Furthermore, uncontrolled urbanization and land-use changes have led to soil degradation, reduced groundwater recharge, and increased flood risks. Hydraulic conductivity and infiltration rate are crucial parameters for mitigating groundwater stress and formulating effective groundwater management strategies in the region. The results of this combined study will help planners and policymakers to design best practices for water resource management in the region, thus improving social and agro-environmental sustainability.

This study aimed to estimate hydraulic conductivity from grain-size analysis, analyze how different grain sizes in the surface soil affect the ability of water to pass through it, investigate infiltration rate, and assess the volume of water that enters aquifers and replenishes groundwater resources.

STUDY AREA

The study area is located in the Erbil basin, a part of the Erbil Plain. It covers an area of about 1,302 km^2, located between 35° 43' 50" to 36° 14' 01" N and 43° 40' 42" to 44° 17' 55" E (Figure 1). Its climate is categorized as dry to semi-arid. The highest temperature is often recorded in late July or early August, and the lowest temperature is typically recorded at the beginning of January and the end of December. The Erbil Basin is characterized by a monthly temperature of 18.94°C, an average of approximately 8.18 hours of sunshine per day, a monthly relative humidity is 47.82%, and a monthly evaporation rate of 200mm[12, 13]. The average annual precipitation in the Erbil basin over the previous 20 years (2000–2020) was approximately 467 mm. Because of its fertile soil and abundant, high-quality groundwater, the Erbil basin is among the most significant basins in the Kurdistan Region/Northern Iraq.

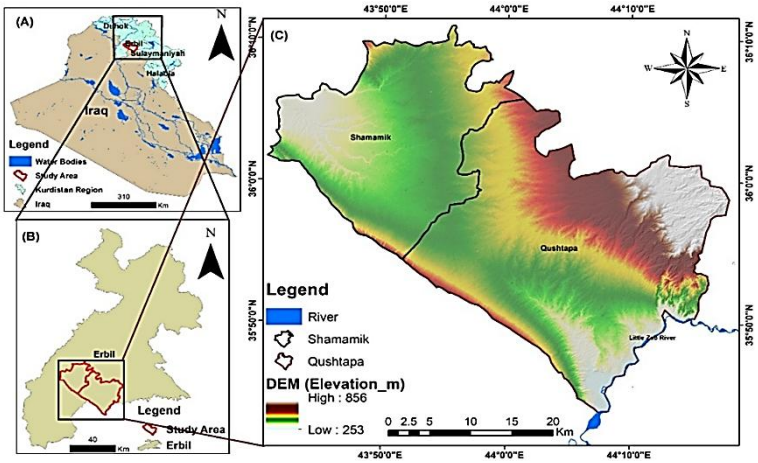

Fig. 1: Location maps of the study area.

Geological Setting

The study area lies within the Low Folded Zone, characterized by limited tectonic activity. Two water bodies delineate the basin; it is bounded to the north by the Greater Zab River and to the south by the Lesser Zab River. Stratigraphically, the major outcrop units are recent alluvium, river terraces, and the Mukdadiya and Bai Hassan Formation deposits (Figure 2). The dominant deposit in the study area is Pleistocene river terraces, consisting of rock and limestone fragments [14]. A recent alluvium deposit is found

in the southern part of the study area, consisting of rock fragments, gravel, silt, and sand, which overlay the Pliocene Mukdadiya and Bai Hassan Formation. The Bai Hassan Formation is exposed to the east and west of the study area and consists of conglomerate, sandstone, and claystone. A few meters of Mukdadiya Formation are exposed in the northwestern parts of the area, consisting of pebbly sandstone, siltstone, and claystone.

- Tectonic Setting

From river valleys to flat alluvial plains, gravel hills, and the Zagros foothill zones, the Erbil basin contains a wide variety of geomorphological and geological features. [15]. Erbil Plain is located in the Law Folded Zone, where drainage patterns have been shaped by several significant anticlines and synclines that align parallel to the Zagros orogeny, which is predominantly oriented from northwest to southeast. It is characterized by significant anticlines and synclines resulting from the collision of the Arabian and Eurasian plates. [14]. The Erbil Basin is situated above a syncline, created by two anticlines: the Permam Dagh anticline to the northeast and the Kirkuk anticline to the southwest.

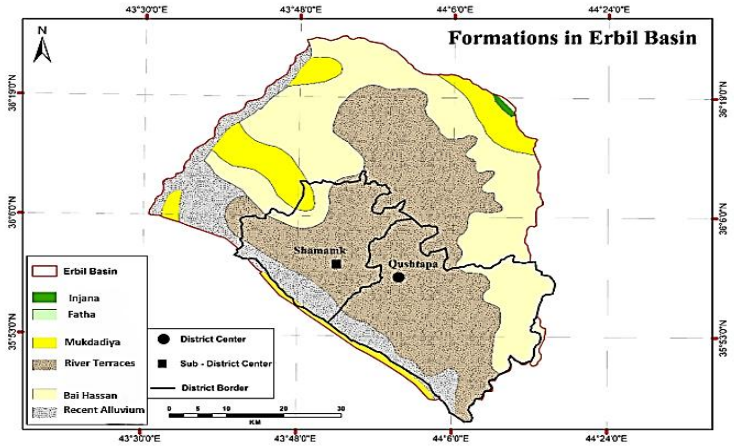

Fig. 2: Formation map of the study area within the Erbil Basin [16].

MATERIALS AND METHODS:

The major steps of data collection and analysis methods have been presented in Figure 3.

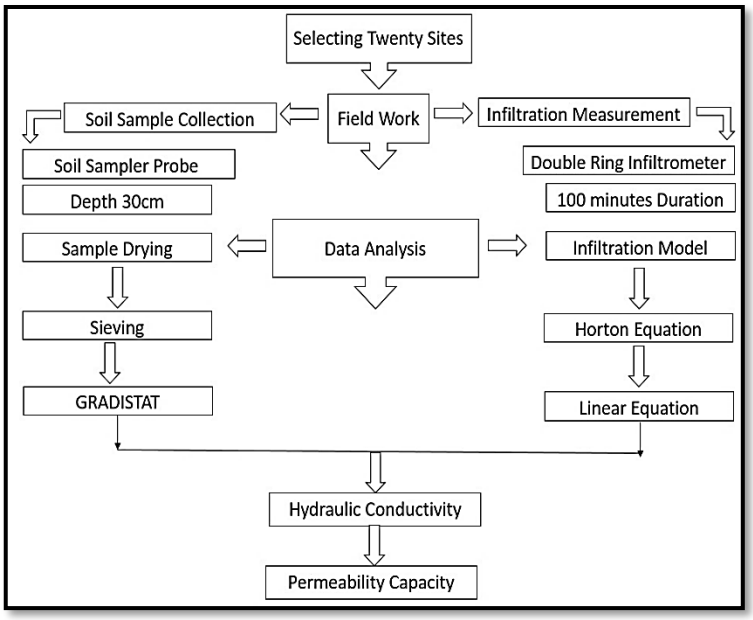

Fig. 3: Schematic overview of methodology and data collection.

Before initiating the infiltration experiment, soil samples were collected at a depth of 30 cm from 20 villages: 10 from the Qushtapa area and 10 from the Shamamik area (Table 1 and Figure 4). All the infiltration tests and soil sample collections were conducted during September 2024. The soil samples were collected with a soil sampler, ensuring the soil surface remained undisturbed. They were dried in an oven at 50°C overnight, weighed, and subjected to grain-size analysis. The size distribution of soil particles expresses the percentage of the soil's weight for each particle size. [17-19]. This analysis was performed using sieves with aperture sizes varying from 2 mm to 0.063 mm at the workshop of the Earth Sciences and Petroleum Department, College of Sciences, Salahaddin University-Erbil. The sieved soil samples were weighed, and the data were entered into the GRADISTAT Version 4.0 grain size analysis statistical program. The effective diameter (d_{10}) for each sample was calculated, and the percentage of gravel, sand, and silt was determined. Additionally, the hydraulic conductivity of each sample was measured using the Hazen method as expressed in equation 1.

DOI: https://doi.org/10.25130/tjps.v31i3.1902

Table 1: Location coordinates of the infiltration field measurement sites.

Sites	Village name	Sub-district	X (UTM)	Y (UTM)	Z (m. a. s. l)
1	Grdlanka	Qushtapa	415601	3963742	304
2	Grda Sor	Qushtapa	422426	3971378	353
3	Dolaza	Qushtapa	413162	3972827	329
4	Qurshaghlu	Qushtapa	402733	3976009	336
5	Azyana	Qushtapa	427209	3973574	424
6	Dola Bakra	Qushtapa	416694	3978146	398
7	Sebiran Ado	Qushtapa	409520	3981740	367
8	Dushiwan	Qushtapa	426077	3982078	488
9	Kardiz	Qushtapa	420273	3984142	451
10	Qucha Blbas	Qushtapa	408651	3990390	366
11	Trpa Spiyan	Shamamik	403979	3982638	338
12	Jdida Lak	Shamamik	397407	3981392	319
13	Helawa	Shamamik	391243	3984258	309
14	Shekh Sherwan	Shamamik	385673	3989176	296
15	Pirdawd	Shamamik	402996	3986652	341
16	Mastawa	Shamamik	392634	3989911	305
17	Daldaghan	Shamamik	400061	3992573	335
18	Dhemat	Shamamik	391889	3995258	301
19	Dustapa	Shamamik	398146	3998393	327
20	Yarmja	Shamamik	395300	3999296	325

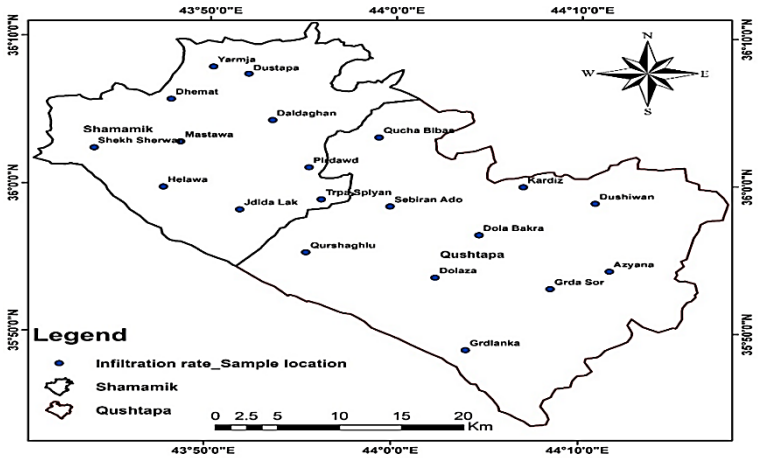

Fig. 4: Location map of infiltration sites.

$K = C*(d_{10})^2$ …….... (1) [20]

where:

K = hydraulic conductivity (m/s)

C = correlation factor based on units [21]

The coefficient in this study was set to 0.01157 [22]

d_{10} = effective grain size diameter (mm).

The infiltration rate experiment has been conducted in 20 villages distributed spatially within the study area, as shown in Figure 4. The experiment was conducted on a flat, dry surface using double-ring infiltrometers; it continued until infiltration reached a steady-state condition. It consists of two rings: an outer ring with a 60 cm diameter and an inner ring with a 30 cm diameter, both 30 cm high. The outer and inner ring indicators were 10cm. Both rings have beveled cutting edges to ease their penetration into the earth's surface [23]. Initially, the outer ring must be

positioned on a flat surface, followed by the inner ring, and the driving plate must be positioned on the top of the rings. Depending on its diameter, the rings will fit over and between the pins on the bottom side of the driving plate, and be driven into the earth using a hand metal hammer until both rings are securely embedded to a depth of 15cm. A manual bubble-level instrument has been adopted to guarantee the ring's uniform entrance into the soil from all sides. A piece of sponge is used to protect the ground surface when pouring the water. Firstly, the outer ring is filled with water until a distinct indicator is reached, then the inner ring is filled with the same labeled indicator. This is to guarantee appropriate infiltration of water and prevent lateral water flow from the inner ring. A 50cm metal ruler was set vertically into the inner ring. The quantity of water entering the soil is measured within the inner ring in centimeters over a period of 100 minutes for each experiment, at designated time intervals (5, 5, 5, 5, 5, 5, 10, 10, 10, 20, and 20 minutes), using a stopwatch. A consistent water level has been maintained in both rings by refilling them to the distinct indicator after each measurement and correcting for any water loss throughout the experiment. During the testing phase, the water depth in the outer ring is maintained to ensure soil saturation in the vicinity of the inner ring, thereby enhancing vertical infiltration beneath it. Additionally, soil permeability is derived from the initial infiltration rate and the steady-state infiltration ratio (F0/Fc), both measured in the field [24].

Infiltration model

The Horton Concept was regarded as fundamental in infiltration investigations. This concept posits that water permeating the soil starts at a uniform rate and diminishes exponentially over time, eventually stabilizing at a specific threshold, indicating a stable state (F_c) [25]. A general flowchart for the infiltration model is shown in Figure 5.

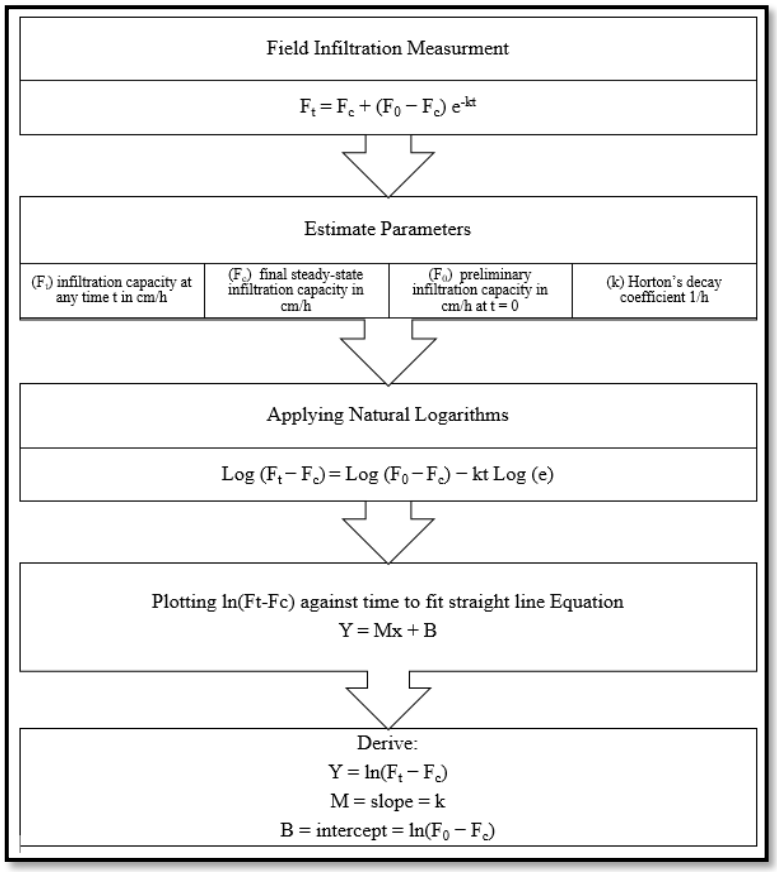

Fig. 5: Flowchart for Horton model.

RESULTS AND DISCUSSION

Grain Size Analysis

This study investigated soil hydraulic conductivity using grain-size analysis. The results of the soil sample analysis and the grain size distribution were recorded. The effective diameter d10, corresponding to 10% of the soil sample being finer by weight, was also determined. The simple correlation analysis between the last measured infiltration rate and effective diameter d_{10} of the soil samples showed a strong positive relationship of approximately 0.847. This meant a direct relationship existed between infiltration rate and soil texture. This outcome aligns with those of [6], who observed that soil with a higher d10 had a higher infiltration rate. Hydraulic conductivity (K) was estimated from the grain size analysis by applying Hazen's formula.

The results indicated that soil samples with a larger d10 value (empirically derived from GRADISTAT) exhibited higher hydraulic conductivity and, consequently, higher infiltration rates (Table 2 and Figure 6). Hydraulic conductivity ranged between $5.3437*10^{-5}$ and $1.0422*10^{-4}$ m/sec with a mean of $6.99*10^{-5}$ m/sec. It's obvious from the hydraulic conductivity prediction map (Figure 6) that the areas that are composed of coarse-grained materials show higher hydraulic conductivity, as Dushiwan Village in the northwestern part of the Qushtapa, which is the Bai Hassan Formation, is the exposed geological formation in the area, exhibiting the highest hydraulic conductivity of $1.0422*10^{-4}$ m/sec since the effective diameter of its soil particles was about 0.0949 mm. In contrast, the lowest hydraulic conductivity, estimated in Dola Bakra Village (located in the center of Qushtapa), was about $5.3437*10^{-5}$ m/sec with a d_{10} of about 0.06796 mm. In contrast, the areas where the river terraces and recent alluvium deposits are dominant geological deposits exhibit lower hydraulic conductivity because they contain a greater proportion of finer materials, including fine sand and very fine sand, as shown in the grain-size distribution (Table 2). The presence of a river channel in Dushiwan Village significantly increased hydraulic conductivity in the area. From a geological perspective, this was attributed to the deposition of coarser-grained sediment, which enhanced permeability and facilitated water infiltration (Figure 7). The results indicated that water velocity was rather high, leading to the deposition of coarser grains. Conversely, regions with lower water velocity had deposits of finer-grained sediment, which reduced soil permeability.

DOI: https://doi.org/10.25130/tjps.v31i3.1902

Table 2: Grain size distribution [17] and the hydraulic conductivity of the soil samples.

Sampling Location	V. Fine Gravel %	V. Coarse Sand %	Coarse Sand %	Medium Sand %	Fine Sand %	V. Fine Sand %	d_{10} (mm)	Hydraulic Conductivity m/sec
Grdlanka	2.2	0.4	13.4	24.6	26.5	32.9	0.08372	$8.1095*10^{-5}$
Grda Sor	1.2	0.7	1.7	7.1	26.1	63.1	0.07387	$6.3135*10^{-5}$
Dolaza	0.3	4.3	14.3	21.9	24.4	34.8	0.07642	$6.7569*10^{-5}$
Qurshaghlu	0.4	1.3	8.3	23.4	24.4	42.1	0.08416	$8.1949*10^{-5}$
Azyana	2.1	3.7	11.8	24.9	27.5	30	0.08049	$7.4958*10^{-5}$
Dola Bakra	0.3	2.8	6.6	8.9	17.7	63.8	0.06796	$5.3437*10^{-5}$
Sebiran Ado	0.2	3.7	3.5	11	22.7	58.9	0.07012	$5.6888*10^{-5}$
Dushiwan	2.5	6	27.7	27.4	18.3	18	0.0949	$1.0422*10^{-4}$
Kardiz	0.7	4.4	16.9	19.1	25.6	33.4	0.0773	$6.9152*10^{-5}$
Qucha Blbas	0.7	4.1	11.6	29	16.8	37.6	0.07784	$7.0103*10^{-5}$
Jdida Lak	0	0.5	10.2	24.9	22.8	41.6	0.07658	$6.7852*10^{-5}$
Trpa Spiyan	0.3	7.8	21.4	21.2	20.2	29.2	0.07753	$6.9547*10^{-5}$
Helawa	0.5	3.5	10.6	19.8	28.1	37.4	0.07704	$6.8669*10^{-5}$
Pirdawd	0.2	1.8	11.3	25.7	23.4	37.6	0.07599	$6.6811*10^{-5}$
Mastawa	0.8	9	23.2	21.6	17.4	28.0	0.07942	$7.2978*10^{-5}$
Shekh Sherwan	1.4	1.9	9	25.2	27.8	34.7	0.08307	$7.9840*10^{-5}$
Daldaghan	0.2	4.1	15.7	22	19.4	38.6	0.07367	$6.2793*10^{-5}$
Dhemat	0.1	4.1	11.6	29	16.8	38.2	0.07784	$7.0103*10^{-5}$
Dustapa	0.1	5.1	9	28.2	20.5	37.1	0.07225	$6.0396*10^{-5}$
Yarmja	0.2	6.4	15.4	17.6	16.8	43.6	0.06938	$5.5693*10^{-5}$

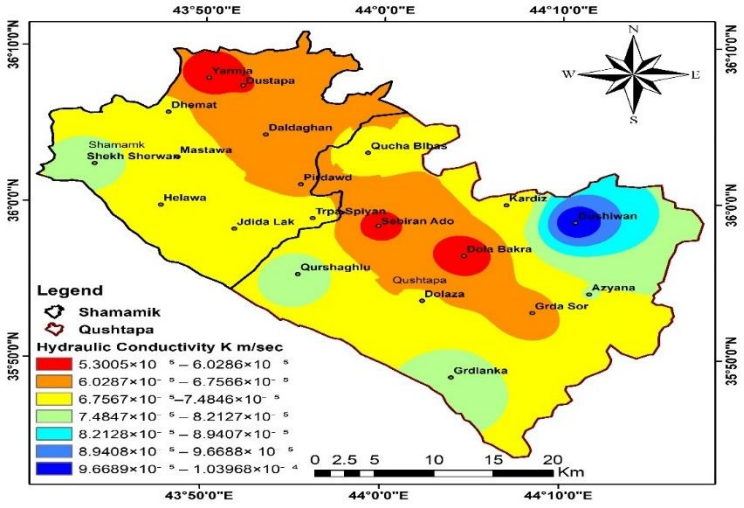

Fig. 6: Hydraulic conductivity prediction map of the topsoil.

DOI: https://doi.org/10.25130/tjps.v31i3.1902

Fig. 7: River channel with gravelly sand sediment.

Infiltration Outcomes

Infiltration rates at 20 sites within the study area were recorded. The infiltration model for the first investigated location is presented in Figures 8 and 9.

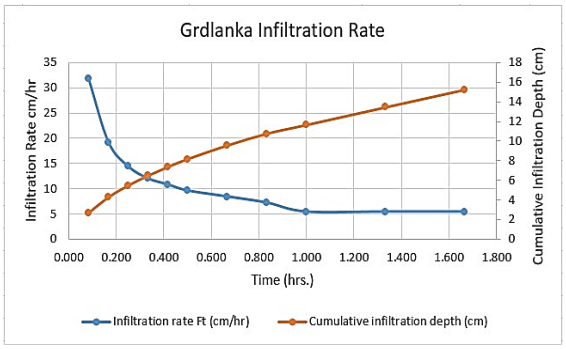

Fig. 8: Infiltration Rate as a Function of Time for Grdlanka Village.

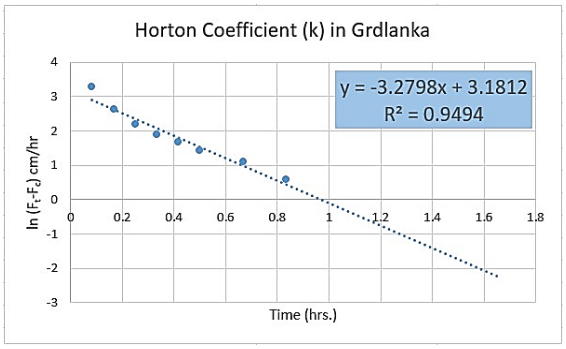

Fig. 9: Determination of k in Horton's Coefficient for Grdlanka Village.

Infiltration started at a high rate and gradually decreased until the soil reached saturation, at which point infiltration reached a steady state (Table 3). The infiltration capacity ranged from 0.9 cm/h (minimum) to 6 cm/h (maximum), with a mean of 3.41 cm/h, recorded in Daldaghan and Dushiwan, respectively. The highest infiltration capacity was recorded in Dushiwan Village in the northeastern part of Qushtapa. The high rate can be attributed to the presence of loose sand in the surficial soil, which may result from erosion of a geological outcrop in this area, thereby enhancing permeability and increasing the speed and movement of water into deeper layers (Figure 10).

The northeastern, southern, and southwestern parts of Qushtapa showed a high infiltration rate, whereas it decreased toward the center of Qushtapa. Daldaghan Village in Shamamik showed the lowest infiltration capacity. The infiltration capacity of soil is highly influenced by soil texture, structure, compaction, moisture content and the presence of organic matter. The results indicate that the soil samples with a greater effective diameter (d10) show higher infiltration capacity than the samples that exhibit less (d_{10}). The maximum infiltration rate is recorded in Dushiwan with a (d_{10}) of about 0.0949 mm, followed by Qurshaghlu, in which the soil's effective diameter is approximately 0.0842 mm. Additionally, Daldaghan shows a minimum infiltration capacity, as the effective diameter of the soil sample is about 0.0773mm. However, a spot west of Shamamik, namely Shekh Sherwan Village, had a high Infiltration capacity, which decreased toward the east and reached its lowest at the northern and northwestern part of Shamamik.

The low infiltration rate at this part was attributed to the fine soil particles; impermeable or clay layers can substantially impede water infiltration. The impact of compaction on infiltration rate is closely related to soil texture; therefore, understanding the influence of soil texture on infiltration rate requires accounting for compaction. Because compaction diminishes pore continuity, thereby impeding water infiltration, it results in surface runoff. Infiltration was measured using the R2 (coefficient of determination), which ranged from 0.7 to 0.98; thus, the field infiltration measurement fit the applied model.

According to [26]A range of R^2 between 70% and 100% indicates a strong connection. Additionally, the field infiltration rate and values derived from the Horton equation were nearly similar (Table 4). All these are indicators of acceptable results. According to [27] (Table 5), The topsoil of the study area is divided into three classes: areas with moderate to rapid, moderate, or slow to moderate infiltration capacity (Table 6 & Figure 11).

The lower rate of infiltration observed in this study in Qurshaghlu, South Western of Qushtapa and Mastawa, Western of Shamamik, in contrast to the rate recorded by [11]can be attributed to vegetation, variation in soil moisture, or climatic conditions, all of which influence the volume of water that permeates the soil.

The findings indicate that soil texture significantly affects infiltration rate. They align with those of [28] who reported that the rate was much greater in loosely compacted soil than in strongly compacted soil, and that the infiltration capacity of soil is influenced by its type and physical characteristics, including texture, bulk density, porosity, and strength. The spatial distribution of both equilibrium infiltration rate and hydraulic conductivity in the study area, as shown in Figures 6 and 11, indicates that there is a direct relationship between both parameters, with the region exhibiting high infiltration rate also exhibiting high hydraulic conductivity, since they are influenced by soil properties such as texture, porosity, and grain size.

Fig. 10: Geological outcrop with loosely compacted Sediment.

DOI: *https://doi.org/10.25130/tjps.v31i3.1902*

Table 3: Infiltration rate during the time in the selected sites.

Incremental depth in interval (cm) in selected sites												
	Yarmja	1.27	0.4	0.3	0.27	0.23	0.2	0.4	0.36	0.33	0.5	0.5
	Dustapa	3.9	1.5	1	0.8	0.6	0.5	0.8	0.5	0.42	0.7	0.7
	Dhemat	1.5	1	0.4	0.35	0.31	0.3	0.6	0.55	0.5	0.7	0.7
	Daldaghan	4.7	1.4	0.9	0.4	0.25	0.23	0.4	0.33	0.3	0.3	0.3
	Mastawa	3.125	1.8	1	0.8	0.6	0.5	0.85	0.8	0.75	1.5	1.5
	Pirdawd	3.8	0.9	0.65	0.6	0.5	0.45	0.7	0.5	0.4	0.8	0.8
	Shekh Sherwan	2.5	1	0.8	0.75	0.7	0.67	1.32	1.2	1	1.8	1.8
	Helawa	2.85	0.75	0.55	0.5	0.43	0.4	0.7	0.6	0.55	1	1
	Jdida Lak	1.8	0.7	0.4	0.33	0.31	0.3	0.57	0.5	0.45	0.8	0.8
	Trpa Spiyan	3.5	1.2	0.8	0.6	0.5	0.4	0.8	0.75	0.7	1.4	1.4
	Qucha Blbas	3	0.95	0.8	0.6	0.5	0.45	0.83	0.8	0.7	1.3	1.3
	Kardiz	3.1	0.9	0.67	0.65	0.65	0.64	0.8	0.7	0.68	1.3	1.3
	Dushiwan	2	0.9	0.78	0.74	0.7	0.65	1.19	1.1	1	2	2
	Sebiran Ado	1.82	1	0.4	0.35	0.33	0.3	0.5	0.48	0.45	0.6	0.6
	Dola Bakra	3.2	1	0.7	0.6	0.4	0.25	0.5	0.45	0.4	0.8	0.8
	Azyana	3.8	2	1	0.8	0.7	0.5	1	1	0.9	1.5	1.5
	Qurshaghlu	3.65	2	1.25	0.9	0.8	0.75	1.45	1.4	1.25	1.9	1.9
	Dolaza	2.4	0.8	0.6	0.4	0.35	0.3	0.6	0.55	0.5	1	1
	Grda Sor	3.1	1.2	0.9	0.6	0.4	0.4	0.6	0.6	0.55	1	1
	Grdlanka	2.65	1.6	1.2	1	0.9	0.8	1.4	1.2	0.9	1.8	1.8
	Time Interval (min)	5	5	5	5	5	5	10	10	10	20	20

DOI: https://doi.org/10.25130/tjps.v31i3.1902

Table 4: The value of Field infiltration rate versus Horton Infiltration Capacity.

Sites	Field Infiltration Measurement F_c (cm/h)	F0 (cm/h)	k (h^{-1})	Horton Equation	Horton Infiltration Capacity F_t (cm/h)	R^2
Grdlanka	5.4	29.47562698	3.2798	$Ft = 5.4+24.0754e^{-3.2724t}$	5.5 er 0.1	0.95
Grda Sor	3	28.21149396	4.8562	$Ft = 3+25.21146e^{-4.8562t}$	3.007 er 0.007	0.92
Dolaza	3	20.47025988	5.4663	$Ft = 3+17.47026e^{-5.4663t}$	3.001er 0.001	0.88
Qurshaghlu	5.7	27.65950334	2.8616	$Ft = 5.7+21.9595e^{-2.8616t}$	5.88 er 0.18	0.79
Azyana	4.5	30.30839948	3.8452	$Ft = 6+12.25458e^{-3.7644t}$	4.54 er 0.04	0.83
Dola Bakra	2.4	35.14007949	6.1703	$Ft = 1.8+32.74008e^{-6.1703t}$	2.4 er 0.0	0.92
Sebiran Ado	1.8	12.55746573	2.9588	$Ft = 1.8+10.7574e^{-2.9588t}$	1.87 er 0.07	0.77
Dushiwan	6	18.25458313	3.7644	$Ft = 6+12.25458e^{-3.7644t}$	6.02 er 0.02	0.89
Kardiz	3.9	29.9782074	5.05	$Ft = 3.9+26.07821e^{-5.05t}$	3.9 er 0.0	0.93
Qucha Blbas	3.9	22.22012166	4.1973	$Ft = 3.9+18.3204e^{-4.1918t}$	3.91 er 0.01	0.9
Jdida Lak	2.4	11.93720056	3.6387	$Ft = 2.4+9.53724e^{-3.639t}$	2.42 er 0.02	0.83
Trpa Spiyan	4.2	33.5296808	6.1314	$Ft = 4.2+29.3294e^{-6.1329t}$	4.2 er 0.0	0.91
Helawa	3	18.85841065	4.1027	$Ft = 3+15.85846e^{-4.1027t}$	3.01 er 0.01	0.89
Pirdawd	2.4	29.56148562	4.5566	$Ft = 2.4+27.1614e^{-4.5527t}$	2.41 er 0.01	0.88
Mastawa	4.5	47.91044151	6.3082	$Ft = 4.5+43.41044e^{-6.3082t}$	4.5 er 0.0	0.99
Shekh Sherwan	5.4	18.69914836	2.9206	$Ft = 5.4+13.2994e^{-2.9213t}$	5.5 er 0.1	0.82
Daldaghan	0.9	26.84554711	4.032	$Ft = 0.9+25.9454e^{-4.0325t}$	0.93 er 0.03	0.8
Dhemat	2.1	9.207851371	2.3881	$Ft = 2.1+7.10784e^{-2.387t}$	2.2 er 0.1	0.7
Dustapa	2.1	42.00493498	4.5398	$Ft = 2.1+39.9044e^{-4.5339t}$	2.12 er 0.02	0.97
Yarmja	1.5	7.56297134	2.8797	$Ft = 1.5+6.06294e^{-2.876t}$	1.54er 0.04	0.77

Table 5: Infiltration Capacity Classification [27].

Equilibrium infiltration rate F_t	Type
> 16 cm/h	Rapid (R)
6-16 cm/h	Moderate - Rapid (M-R)
2-6 cm/h	Moderate (M)
0.5-2 cm/h	Slow – Moderate (S-M)
0.12-0.5 cm/h	Slow (S)
< 0.12 cm/h	Very Slow

Table 6: Study area Classification based on Infiltration Capacity [27].

Village Name	Infiltration Capacity Classification	Village Name	Infiltration Capacity Classification
Grdlanka	M	Jdida Lak	M
Grda Sor	M	Trpa Spiyan	M
Dolaza	M	Helawa	M
Qurshaghlu	M	Pirdawd	M
Azyana	M	Mastawa	M
Dola Bakra	M	Shekh Sherwan	M
Sebiran Ado	S-M	Daldaghan	S-M
Dushiwan	M-R	Dhemat	M
Kardiz	M	Dustapa	M
Qucha Blbas	M	Yarmja	S-M

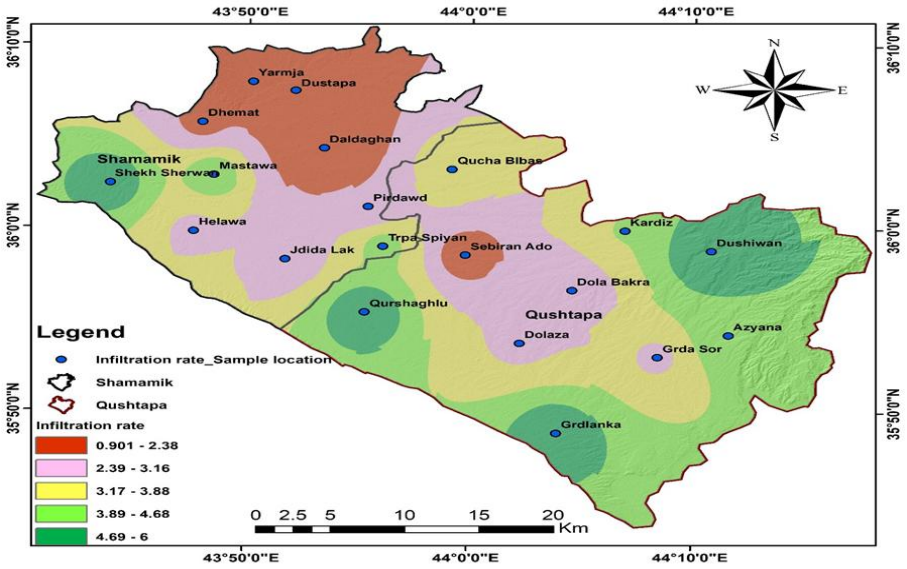

Fig. 11: Equilibrium infiltration rate map.

Permeability capacity

Soil permeability is a measure of how easily water can pass through the soil. It is influenced by several parameters, including void ratio, intergranular pore dispersion, and saturation degree [29]. Soil permeability is derived from the initial infiltration rate and the steady-state infiltration ratio (F0/Fc), both measured in the field [24]. The permeability capacity of the tested sites is shown in Table 7. The F_0/Fc ratio indicates changes in infiltration rates over time, influenced by soil surface conditions. High values indicate rapid

decline, while low values suggest stable infiltration behavior, often associated with uniform, well-structured soils with better permeability, as shown in Figure 12. In this study, the initial infiltration rate ranged from 7.56 to 47.91 cm/h, while the constant infiltration rate ranged from 0.9 to 6 cm/h. The soil permeability at each location was measured (Table 8), and the results showed that the study area had moderate to high permeability. In locations with low infiltration rates, the F_0/F_c ratio was high, indicating that the soil initially absorbs water quickly and then rapidly loses its ability to do so. Additionally, locations with low infiltration capacity demonstrated insufficient water absorption early. This may have arisen from soil moisture content and/or compacted layers or surface sealing, which impede water infiltration at the surface, where fine-grain soil retains higher moisture content than coarse-grain soil [30]. Nevertheless, deeper soil strata or areas with extensively connected pores might exhibit elevated permeability. Consequently, it can be inferred that although infiltration capacity was low, permeability remained high due to well-interconnected pores in the deeper layers, which facilitated water movement through the soil over time.

Table 7: Permeability Indication Ratio [24].

F_0/F_c Ratio	Permeability Capacity
> 5	High Permeability
3-5	Moderate Permeability
<3	Low Permeability

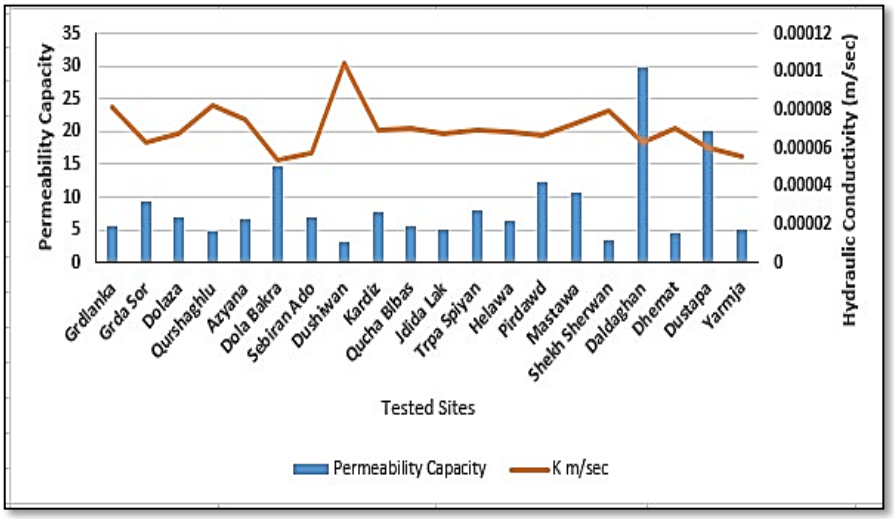

Fig. 12: Relationship between permeability capacity(F_0/F_c) and hydraulic conductivity.

Table 8: Permeability Indication ratio in the study area [24].

Village Name	F_0/F_c Ratio	Permeability Capacity
Grdlanka	29.475/5.4 = 5.458	High Permeability
Grda Sor	28.211/3 = 9.404	High Permeability
Dolaza	20.470/3 = 6.823	High Permeability
Qurshaghlu	27.660/5.7 = 4.853	Moderate Permeability
Azyana	30.308/4.5 = 6.735	High Permeability
Dola Bakra	35.140/2.4 = 14.642	High Permeability
Sebiran Ado	12.557/1.8 = 6.976	High Permeability
Dushiwan	18.254/6 = 3.042	Moderate Permeability
Kardiz	29.978/3.9 = 7.687	High Permeability
Qucha Blbas	22.220/3.9 = 5.697	High Permeability
Jdida Lak	11.937/2.4 = 4.974	Moderate Permeability
Trpa Spiyan	33.529/4.2 = 7.983	High Permeability
Helawa	18.858/3 = 6.286	High Permeability
Pirdawd	29.561/2.4 = 12.317	High Permeability
Mastawa	47.910/4.5 = 10.646	High Permeability
Shekh Sherwan	18.699/5.4 = 3.463	Moderate Permeability
Daldaghan	26.845/0.9 = 29.828	High Permeability
Dhemat	9.208/2.1 = 4.385	Moderate Permeability
Dustapa	42.005/2.1 = 20.002	High Permeability
Yarmja	7.562/1.5 = 5.0419	High Permeability

CONCLUSION

1. The highest hydraulic conductivity was observed northeast of Qushtapa due to the greater effective diameter, while the lowest was revealed in the central part of the Qushtapa area, attributed to a smaller effective diameter
2. Most of the examined locations had moderate infiltration capacities, which were proportionally elevated in areas with greater effective soil grain diameter.
3. The northeast and south-southwestern parts of Qushtapa showed higher infiltration capacity, in addition to the west of Shamamik, due to the dominance of coarse-grained soil
4. There is a direct relationship between soil texture, its permeability, and its capacity to allow water infiltration.
5. Generally, the soil of the study area showed moderate to high permeability.
6. The field-measured infiltration rates aligned well with the rates predicted by Horton's equation.

Conflict of interest: The authors declared no conflicts of interest.

Sources of funding: This research did not receive any specific grant from funding agencies in the public, commercial, or not-for-profit sectors.

Author contributions: The authors contributed equally to the study.

REFERENCE

1. Epting J, Vinnå LR, Piccolroaz S, Affolter A, Scheidler S. Impacts of climate change on Swiss alluvial aquifers–A quantitative forecast focused on natural and artificial groundwater recharge by surface water infiltration. Journal of Hydrology X. 2022;17:100140. https://doi.org/10.1016/j.hydroa.2022.100140

2. Mgolozeli S, Nciizah AD, Wakindiki II, Mudau FN, Onwona-Agyeman S. Investigation of infiltration and runoff rate on agri-mats using a laboratory rainfall simulation study. Communications in Soil Science and Plant Analysis. 2023;54(8):1005-14.

https://doi.org/10.1080/00103624.2022.2137187
3. Kuma HG, Feyessa FF, Demissie TA. Assessing the impacts of land-use/land-cover changes on hydrological processes in Southern Ethiopia: The SWAT model approach. Cogent Engineering. 2023;10(1):2199508. https://doi.org/10.1080/23311916.2023.2199508
4. Bittelli M, Campbell GS, Flury M. Characterization of particle-size distribution in soils with a fragmentation model. Soil Science Society of America Journal. 1999;63(4):782-8. https://doi.org/10.2136/sssaj1999.634782x
5. Basset C, Abou Najm M, Ghezzehei T, Hao X, Daccache A. How does soil structure affect water infiltration? A meta-data systematic review. Soil and Tillage Research. 2023;226:105577. https://doi.org/10.1016/j.still.2022.105577
6. Mutasher AKA. Determining the Infiltration Rate by Using a Double-Ring Infiltrometer in AL-Jadwal Al-Gharbi District, Karbala, Iraq.
7. Gebul MA. Simplified approach for the determination of parameters for Kostiakov's infiltration equation. Water Practice & Technology. 2022;17(11):2435-46. https://doi.org/10.2166/wpt.2022.142
8. Netzer L, Kurtzman D, Ben-Hur M, Livshitz Y, Katzir R, Nachshon U. Novel approach to roof rainwater harvesting and aquifer recharge in an urban environment: Dry and wet infiltration wells comparison. Water Research. 2024;252:121183. https://doi.org/10.1016/j.watres.2024.121183
9. Smith RE. Infiltration theory for hydrologic applications: American Geophysical Union; 2002.
10. Shwani SO. Hydrogeology and Hydrochemistry of Bashtapa Sub-Basin in Erbil Governorate, Kurdistan Region, Iraq. Erbil: Salahaddin University, Geology Department; 2008.
11. Bapeer GB, Surdashy AM, Hassan KM. Infiltration rates of soils in some locations within Erbil Plain, Kurdistan Region, North Iraq. Iraqi Bulletin of Geology and Mining. 2010;6(2):127-37.
12. Mustafa JS, Mawlood DK. Hydrological study and water budget assessment of the Erbil basin, Kurdistan Region, Iraq. 2024. https://doi.org/10.1016/j.asej.2024.102781
13. Hamad R. Erbil Basin Groundwater Recharge Potential Zone Determination Using Fuzzy-Analytical Hierarchy Process (AHP) in North Iraq. Tikrit journal for agricultural sciences. 2022;22(3):175-90. https://doi.org/10.25130/tjas.22.3.20
14. Jassim SZ, Goff JC. Geology of Iraq. st E, editor. Prague and Brno: Dolin, Prague and Moravian Museum; 2006.
15. Dizayee R. Groundwater Degradation and Sustainability of the Erbil Basin, Erbil, Kurdistan Region, Iraq. Fort Worth, TX: Texas Christian University; 2014.
16. Mustafa JS, Mawlood DK. Assessment of the Groundwater in Erbil Basin with Support of Visual MODFLOW. Journal of Ecological Engineering. 2024;25(4). https://doi.org/10.12911/22998993/184184
17. Folk RL, Ward WC. Brazos River bar [Texas]; a study in the significance of grain size parameters. Journal of Sedimentary Research. 1957;27(1):3-26.
18. Abboud MR, al-Obeidi AA-H. Geotechnical properties of soil for selected sites in Kirkuk city. Tikrit Journal of Pure Science. 2016;21(4):97-105. https://doi.org/10.25130/tjps.v21i4.1060
19. Hassan IM, Abood MR, Kadhim LS. Validity of the Lower Zab River Sediments for Road and Asphalt Works-Southwest of Kirkuk/Northern Iraq. Tikrit Journal of Pure Science. 2023;28(2). https://doi.org/10.25130/tjps.v28i2.1334
20. Price W, Potter A, Thomson TK, Smith G, Hazen A, Beardsley R. Discussion on dams on sand foundations. Transactions of the American Society of Civil Engineers. 1911;73(3):190-208.
21. Fetter C, Rayne T. Solution Manual to Accompany Applied Hydrogeology: Macmillan College; 1994.
22. Svensson A. Estimation of hydraulic conductivity from grain size analyses: A

comparative study of different sampling and calculation methods focusing on Västlänken. Göteborg, Sweden: Chalmers University of Technology; 2014.

23. ASTM. Standard test method for infiltration rate of soils in the field using a double-ring infiltrometer. West Conshohocken, PA: American Society for Testing and Materials; 2003. Contract No.: ASTM D3385-03.

24. McCuen RH. Hydrologic analysis and design. Englewood Cliffs, NJ: Prentice-Hall; 1989.

25. Horton RE, editor. An approach toward a physical interpretation of infiltration capacity. Soil science Society of America proceedings; 1940: Madison.

26. Champatiray A. Experimental study for determination of infiltration rate of soils in field using double ring infiltrometer 2014.

27. Nikolov SJB. Rainfall erosion in northern Iraq. Iraq: Unspecified Publisher; 1983.

28. Cleophas F, Isidore F, Musta B, Ali BM, Mahali M, Zahari N, et al., editors. Effect of soil physical properties on soil infiltration rates. Journal of physics: conference series; 2022: IOP Publishing.

29. Elhakim AF. Estimation of soil permeability. Alexandria Engineering Journal. 2016;55(3):2631-8. https://doi.org/10.1016/j.aej.2016.07.034

30. Abdullah Fouad Ibrahim Al B, Amera Ismail Hussain K. Study Some Physical Properties Of Soil in Tuz Khormatu, North of Iraq. Tikrit Journal of Pure Science. 2016;21(7):129-42. https://doi.org/10.25130/tjps.v21i7.1120